

Supporting Information

Chlorine Corrosion of Ubiquitous Rust Led to Low-Cost, Efficient and Free-Standing Electrocatalysts for Overall Water Splitting

Emei Zheng^{a}, Qi Zheng^b, Mengfei Liu^c, Sheng Fu^c, Lei Liang^{c*}*

*Corresponding author

E-mail: zhengemei@163.com and LEI.LIANG@SLENERGY.COM

†These authors contributed equally to this work

Experiment Section

Corrosive stainless steel (RSS): Firstly, stainless steel (SS, 304, 1*2 cm⁻²) was washing with deionized water and ethanol by sonication for several times. Afterward, it was immersed into 25 mL of alkaline solution containing 5 mL of NH₃·H₂O. Then, it was sealed in autoclave and heated at 200°C for 5 h. After washing with water, the plate can be directly used as the working electrode

Rusted stainless steel corroded by chloride ion (RSS-LDH): The rusted stainless steel prepared above was put into a container containing NaCl (0.5 M), and let the container react for 24 h at 25°C to ensure that the stainless steel surface can react completely. After that, the collected RSS-LDH was washed three times with deionized water. Finally, dry in a 60°C oven overnight.

Materials characterizations

Morphological analysis of anode microstructure was carried out using optical microscope, scanning electron microscope (SEM, JEOL-6700F) and transmission electron microscope (TEM, JEOL JEM-2100F). For elemental analysis, X-ray diffraction (XRD) data is measured by a Bruker D8 Advance with Cu-K α X-ray radiation ($\lambda = 0.154056$ nm), using an operating

voltage of 40 kV and X-ray photoelectron spectroscopy (XPS, Thermo ESCALAB 250Xi) with a monochromatic Al K α source were employed.

Electrochemical measurements

All electrochemical measurements were carried out on 760E electrochemical workstation (Shanghai CH instrument). Electrocatalytic performance for OER and HER were measured in a three-electrode cell, using Pt wire as counter electrode for OER, graphite rod as counter electrode for HER, and Ag/AgCl electrode as reference electrode. The measured potential refers to RHE, $ERHE = E_{Ag/AgCl} + 0.059 \cdot pH + E^{\theta}_{Ag/AgCl}$.

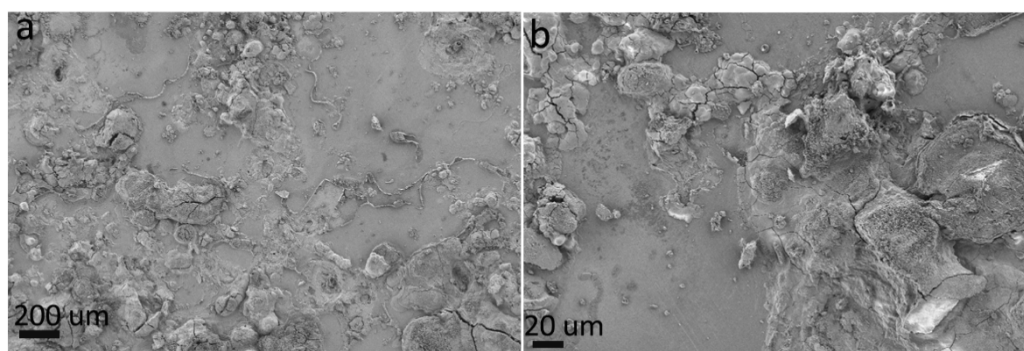


Figure S1. The SEM images for the RSS.

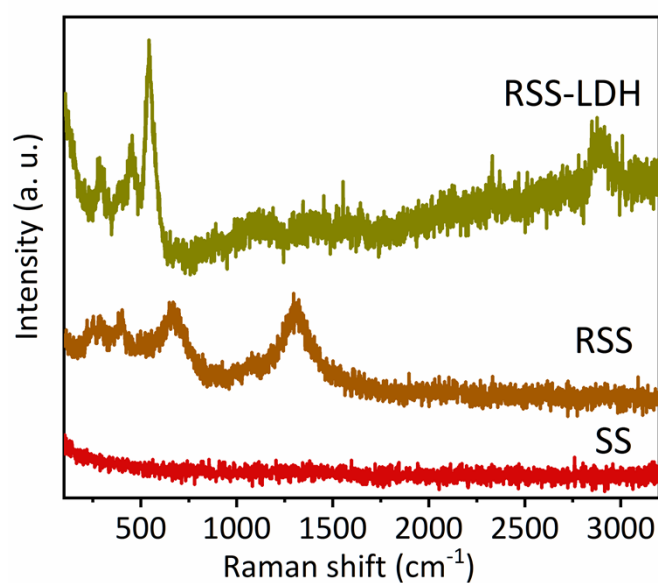


Figure S2. Raman spectra of SS, RSS and RSS-LDH.

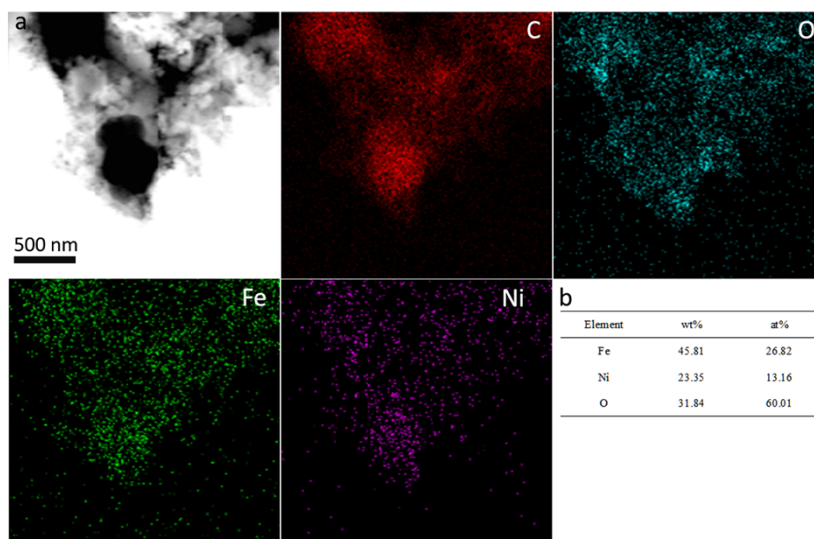


Figure S3. SEM images (a, b), TEM image (c), Elemental maps (d), and HAADF-STEM image (e) for RSS-LDH.

Table S1. Contents of Fe, Ni, Cr and O of the as-prepared samples based on the XPS results.

| Materials | Fe (at%) | Ni (at%) | Cr (at%) | O (at%) |
|-----------|----------|----------|----------|---------|
| SS | 16.33 | 0.52 | 13.11 | 70.04 |
| RSS | 14.23 | 0.85 | 4.12 | 80.8 |
| SS-LDH | 15.12 | 7.91 | 1.84 | 75.05 |
| RSS-LDH | 16.21 | 7.93 | 1.82 | 74.04 |

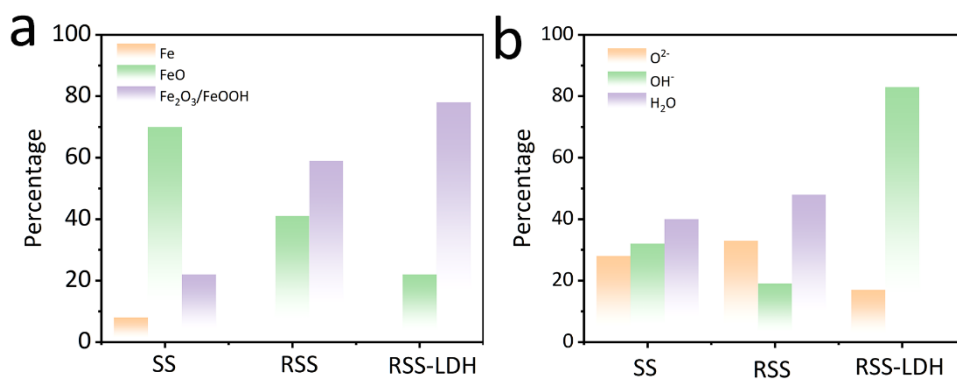


Figure S4. The relative ratios of Fe (a), Ni (b) and O (c) species for SS, RSS and RSS-LDH.

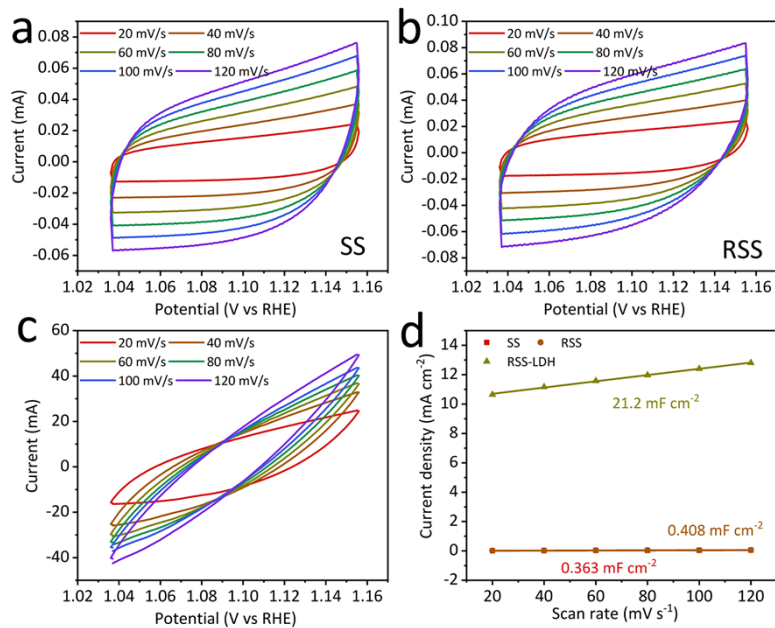


Figure S5. (a, b, c) CV curves recorded at different scan rates in 0.1 M KOH electrolyte. (d) Double layer charging current plotted against scan rate over SS, RSS and RSS-LDH.

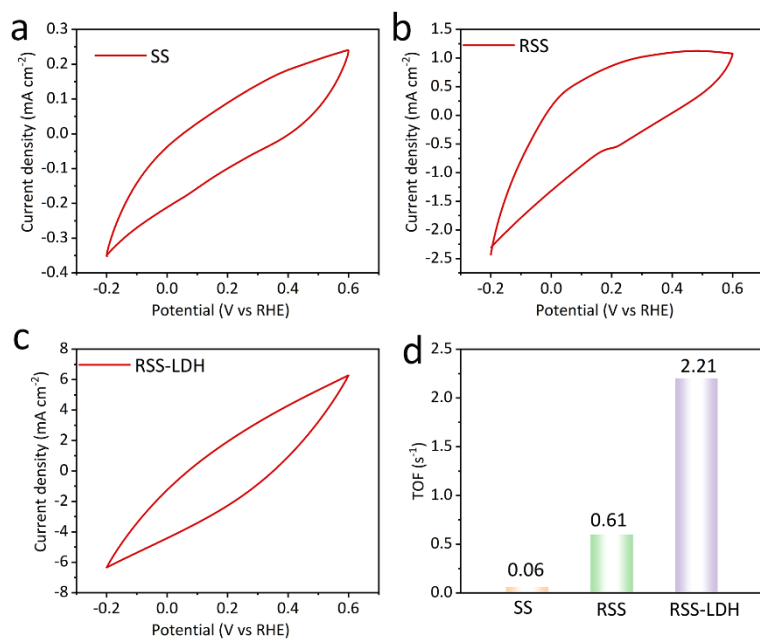


Figure S6. CV curve for (a) SS, (b) RSS and (c) RSS-LDH recorded between -0.2 and 0.6 V vs. RHE in PBS (pH=7) at a scan rate of 50 mV s⁻¹. (d) Comparison of TOF value of RSS-LDH, RSS and SS.

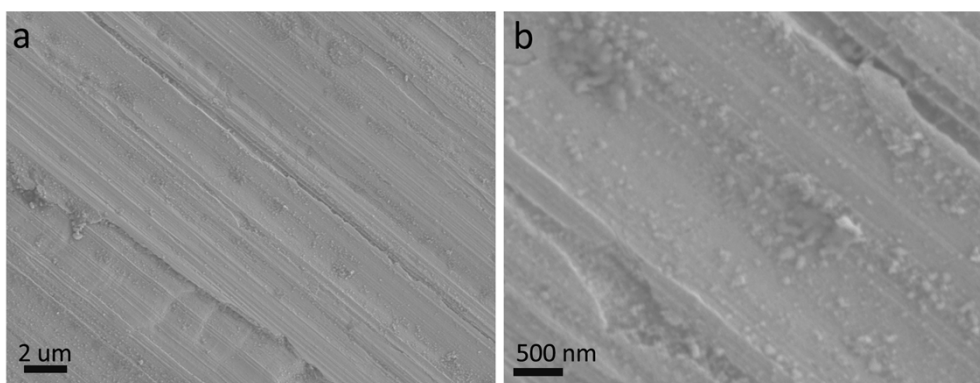


Figure S7. (a) SEM images of SS corroded in the aqueous solution of Na_2SO_4 (0.5 M). (b) SEM images of SS in the aqueous solution of NaNO_3 (0.5 M).

In order to reveal the role of Cl^- ions in the corrosion reaction, Na_2SO_4 (0.5 M) and NaNO_3 (0.5 M) were used instead of NaCl (0.5 M) respectively, and they reacted with SS under the same conditions. However, no nanosheets grow on the surface of stainless steel, which indicates that the corrosion of chloride ions plays an important role in the formation of hydroxide nanosheets (Figure S6).

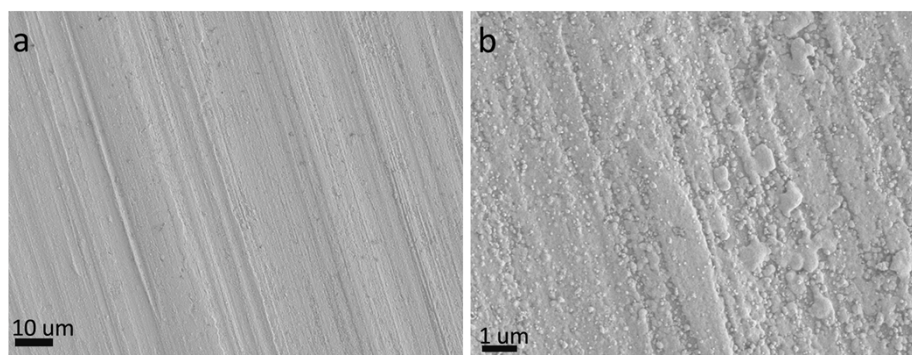


Figure S8. (a, b) SEM images for SS corroded in NaCl (0.5 M) without O_2 .

On the other hand, oxygen (O_2) also shows an important role in the process of metal corrosion. Therefore, in order to prove that O_2 is also an indispensable part in this reaction, N_2 is used to degas NaCl solution for 30 minutes. Then, the container after the reaction was put into a glove box filled with N_2 , and SS was put into the container after the reaction for 24 hours (Figure S7). However, the surface of SS remains clean, indicating that O_2 is also an important part in the process of producing polymetallic hydroxides. According to the results, it can be concluded that

the generated hydroxide nanosheets are generated under the synergistic effect between Cl^- ions and O_2 .

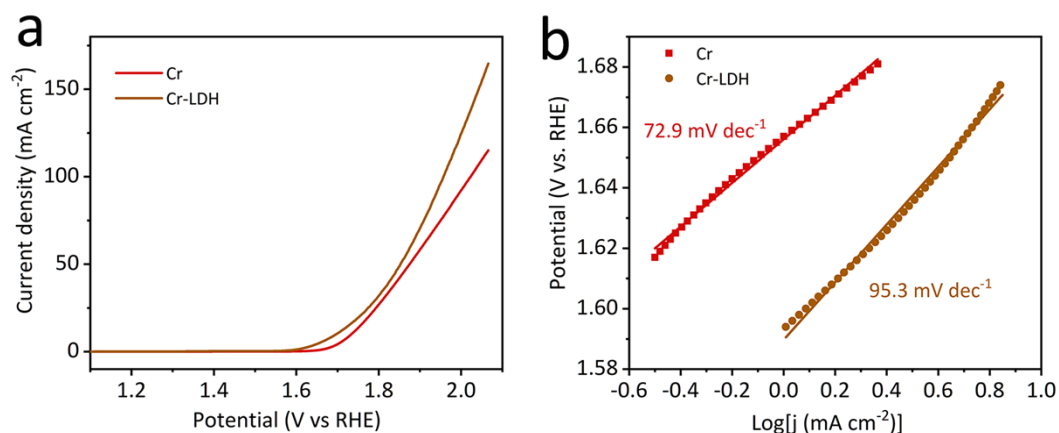


Figure S9. OER polarization curve (a) and EIS (b) of Cr and Cr-LDH in 1 M KOH solution (Inset: the corresponding Tafel plots).

As shown in Fig. S8, compared with RSS-LDH, Cr-LDH shows a larger overpotential (680 mV) to provide a current density of 100 mA cm^{-2} and a Tafel slope (95.3 mV dec^{-1}), which is due to the low activity of the intrinsic active site of Cr-LDH, indicating that Cr substance has little contribution to the enhancement of OER performance at RSS-LDH electrode.

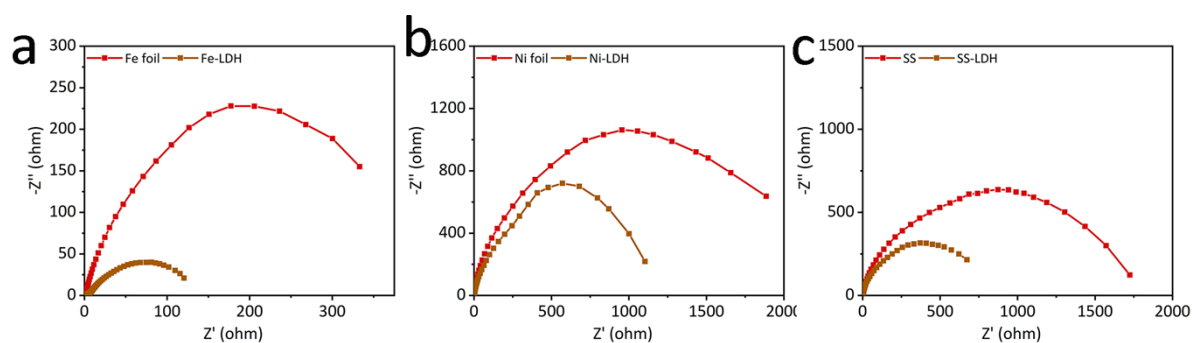


Figure S10. (a-c) EIS of Fe foil, Fe-LDH, Ni foil, Ni-LDH, SS and SS-LDH in 1 M KOH solution.

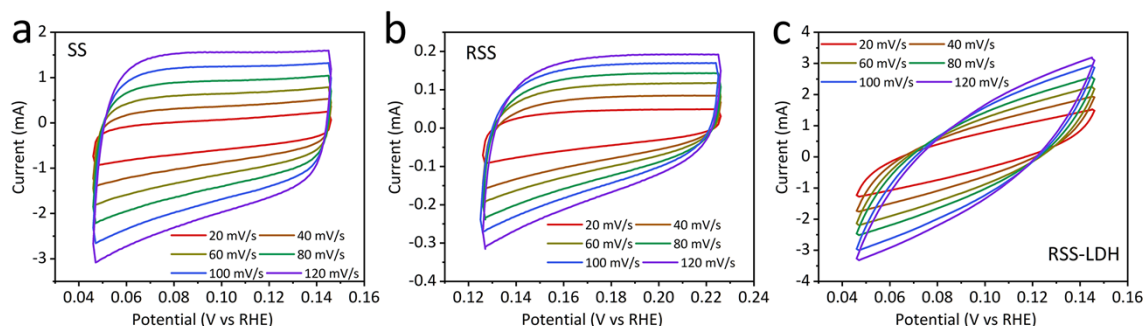


Figure S11. Non-Faradaic scan for double-layer capacitance. Cyclic voltammetry for OER (a-d) and HER (e-h).

Table S2. Comparison with some representative electrocatalysts for OER recently reported.

| Catalysts | Electrolyte solution | Overpotential (mV) | Tafel slope (mV·dec ⁻¹) | Reference |
|----------------------------------|----------------------|---|-------------------------------------|--|
| NiCoFe-LDHs | 1.0 M KOH | 288@10 mA·cm ⁻² | 92 | ACS Catal. 2020, 10, 9, 5179–5189 |
| NiFe-LDH/FeCoS ₂ /CFC | 1.0 M KOH | 190@10 mA·cm ⁻² | 56 | J Mater Sci 2020, 55, 16625–16640 |
| NiCo-LDH/NF | 1.0 M KOH | 271 @10 mA·cm ⁻² | 72 | Dalton Trans., 2017, 46, 8372-8376 |
| FeCoNi-LTH/NiCo2O4/CC | 1.0 M KOH | 302@50 mA·cm ⁻² | 71.5 | ACS Appl. Mater. Interfaces 2017, 9, 42, 36917–36926 |
| Fe–Ni LDH/MOF-b2 | 1.0 M KOH | 255@10 mA·cm ⁻² | 24 | Nanoscale, 2020,12, 14514-14523 |
| NiFe@LDH/NF | 1.0 M KOH | 260@10 mA·cm ⁻² | 76 | Energy Fuels 2024, 38, 14, 12888–12899 |
| RSS-LDH | 1.0 M KOH | 137@10 mA·cm ⁻² 340@100 mA·cm ⁻² | 45.6 | This work |

Table S3. Comparison with some representative electrocatalysts for HER recently reported.

| Catalysts | Electrolyte solution | Overpotential (mV) | Tafel slope (mV·dec ⁻¹) | Reference |
|---------------------------------|----------------------|----------------------------|-------------------------------------|---|
| NiFe-LDH/VSe ₂ | 1.0 M KOH | 168@10 mA·cm ⁻² | 98 | Int. J. Hydrogen Energ., 2024, 71, 1456-1467 |
| NF/Mo-NiFe LDH/NiS _x | 1.0 M KOH | 169@10 mA·cm ⁻² | 119.8 | J. Colloid Interface Sci., 2024, 664, 980-991 |

| | | | | |
|---------------------------|-----------|---|------|--|
| S-NiFe LDH/MXene@NF | 1.0 M KOH | 209@50 mA·cm ⁻² | 113 | ACS Sustainable Chem. Eng. 2024, 12, 31, 11520–11530 |
| FeNiCoAlP | 1.0 M KOH | 134@20 mA·cm ⁻² | 80 | Int. J. Hydrogen Energ., 2021, 46, 36731-36741 |
| MoO ₃ /NiFe-NF | 1.0 M KOH | 85@10 mA·cm ⁻² | 97.4 | Small 2024, 20, 2307797 |
| RSS-LDH | 1.0 M KOH | 137@10 mA·cm ⁻² 310@100 mA·cm ⁻² | 79.7 | This work |

Table S4 Fitting results of Nyquist plots for HER.

| Electrodes | Rs(Ω) | Rct(Ω) |
|------------|-------|--------|
| SS | 1.54 | 152 |
| RSS | 1.2 | 30 |
| RSS-LDH | 0.93 | 8.4 |

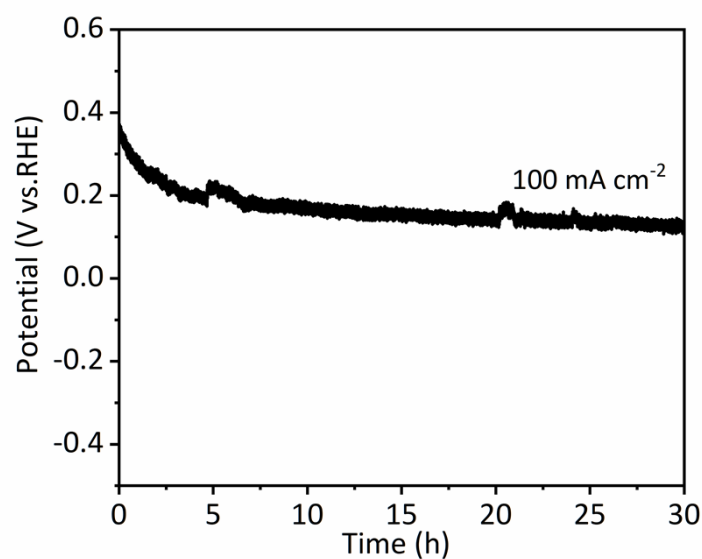


Figure S12. Chronopotentiometry of RSS-LDH at 100 mA·cm⁻² for HER.

Table S5. Comparison of some representative catalysts for overall water splitting recently reported.

| Catalysts | Electrolyte solution | Overall voltage (V) at j=10 mA·cm ⁻² | Reference |
|-----------|----------------------|---|-----------|
| | | | |

| | | | |
|---|---------|------|---|
| CFeCoNiP/NF | 1 M KOH | 1.52 | Journal of Materials Chemistry A 2020, 8, 9939. |
| Fe ₃ C-Co/NC | 1 M KOH | 1.5 | Small 2018, 14, 1704073. |
| Ni _{1-x} Fe _x - LDH/NF | 1 M KOH | 1.59 | ACS Applied Materials & Interfaces 2018, 10, 42453 |
| Ru-CoV- LDH@NF | 1 M KOH | 1.50 | ChemSusChem, 14, 2021, 730-737 |
| MoS ₂ /NiFe LDH | 1 M KOH | 1.57 | Nano Lett. 2019, 19, 4518– 4526 |
| NiFe- LDH@NiCoP | 1 M KOH | 1.57 | Advanced Functional Materials 2018, 28, 1706847 |
| RSS-LDH | 1 M KOH | 1.42 | This work |
